Composite Materials for Implant Applications in the Human Body

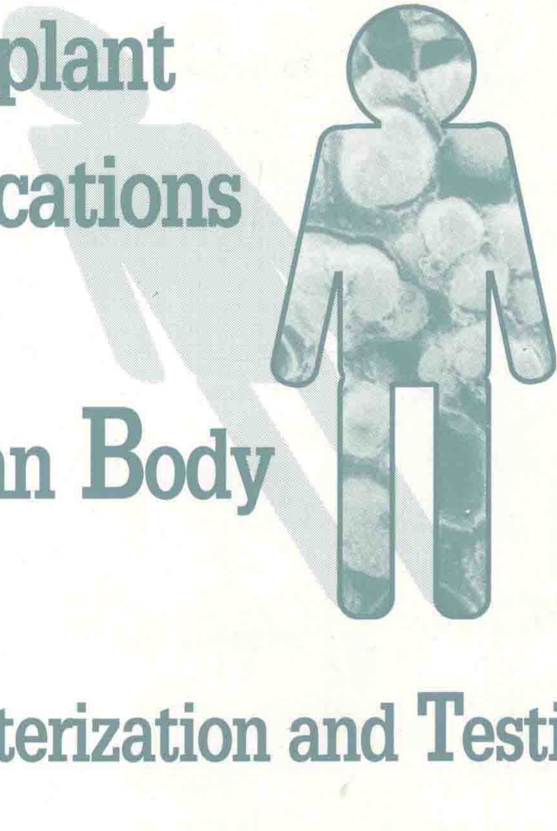

Characterization and Testing

Jamison/Gilbertson EDITORS

STP 1178

STP 1178

Composite Materials for Implant Applications in the Human Body: Characterization and Testing

Russell D. Jamison and Leslie N. Gilbertson, editors

ASTM Publication Code Number (PCN)
04-011780-54

ASTM
1916 Race Street
Philadelphia, PA 19103

Library of Congress Cataloging-in-Publication Data

Composite materials for implant applications in the human body: characterization and testing / Russell D. Jamison and Leslie N. Gilbertson, editors.
(STP; 1178)
"Contains papers presented at the symposium . . . held in San Diego, CA, on 6 Nov. 1991 . . . sponsored by ASTM Committee F-4 on Medical and Surgical Materials and Devices"—Foreword.
Includes bibliographical references and indexes.
ISBN 0-8031-1852-X
1. Biomedical materials—Congresses. 2. Composite materials—Congresses. 3. Orthopedic implants—Congresses. I. Jamison, Russell D. II. Gilbertson, L. N. III. ASTM Committee F-4 on Medical and Surgical Materials and Devices. IV. Series: ASTM special technical publication; 1178.
R857.M3C6 1993
617.3'07—dc20 92-44626
CIP

Peer Review Policy

Each paper published in this volume was evaluated by three peer reviewers. The authors addressed all of the reviewers' comments to the satisfaction of both the technical editor(s) and the ASTM Committee on Publications.

The quality of the papers in this publication reflects not only the obvious efforts of the authors and the technical editor(s), but also the work of these peer reviewers. The ASTM Committee on Publications acknowledges with appreciation their dedication and contribution to time and effort on behalf of ASTM.

Printed in Philadelphia, PA
February 1993

Foreword

This publication, *Composite Materials for Implant Applications in the Human Body: Characterization and Testing*, contains papers presented at the symposium of the same name held in San Diego, CA on 6 Nov. 1991. The symposium was sponsored by ASTM Committee F-4 on Medical and Surgical Materials and Devices. Russell D. Jamison of Smith & Nephew Richards, Inc., in Memphis, TN and Leslie N. Gilbertson of Zimmer, Inc., in Warsaw, IN presided as symposium chairman and co-chairman, respectively, and are the editors of the resulting publication.

Contents

Overview

Since portions of the human body are composite structures, the progression towards the use of composite materials for application in the human body is natural. Because the properties of materials and interfaces in the body are unique, it is difficult to duplicate these properties or even to accommodate them without considering the potential advantages of engineered composite materials custom tailored mechanical properties. The bulk of papers in this symposium are concerned with orthopaedic applications. This is not unusual for three reasons: (1) the ASTM Committee F-4 on Surgical Implants that sponsored this symposium is a primary source worldwide for standards related to orthopaedic materials and devices; (2) the market for orthopaedic products is well-established and materials conscious; and (3) the replacement of the unique properties of bone-in-bone interfaces appears to be an excellent application for structural composites. Despite the optimism about the potential of orthopaedic applications of composite, the emphasis of many of these papers is caution. Orthopaedic prosthetic devices are nonredundant systems that are not easily replaced. Failure of a single component in a system or a material could lead to loss of function of the device and require a revision operation. Consequently, many of the test methods relate to the long-term viability of the composite materials and devices.

The two papers by Maharaj and Jamison highlight two potential problems for a stemmed femoral total hip replacement fabricated from structural composites. The paper entitled, "Intraoperative Impact: Characterization and Laboratory Simulation on Composite Hip Prostheses," covers potential effects of impacts that are typical of surgical implantation techniques for femoral stems. The effect of these impact loads must be considered in terms of the potential damage they may cause to the composite material. Thus, impact loading should be a part of a representative environmental conditioning step, prior to any long life fatigue evaluation of a prosthesis.

The paper, "Creep Testing of a Composite Material Human Hip Prosthesis," points up another problem related to the viscoelastic nature of the polymer matrix of many polymer fiber composites. Under continuing load there can be plastic deformations that occur in the viscoelastic polymeric matrix. Although most of a femoral component in a Total Hip Replacement (THR) is supported by bone that provides additional resistance to creep, the portions of the prosthesis above the bone will never see any additional support, and consequently could be subject to significant amounts of creep. Developing methods to study creep in simulated applications and determining if it represents a problem in long-term application of the material to the total hip prosthesis are significant steps in the design of structural composite material implants. The paper by Humphrey and Gilbertson, "Fatigue Testing of Femoral Hip Prostheses with a Two Beam Simulated Femoral Bone Support Fixture," attempts to find an improved simulation method for the fatigue testing of composite hip prosthesis. One of the potential advantages of a composite THR femoral stem would be to achieve elastic properties closer to those of living bone. Such a low modulus implant, however, severely overburdens many of the fatigue methods currently used to evaluate the long-term fatigue resistance of hip stems. Providing a method to adequately evaluate the long-term fatigue resistance of composite femoral stems is another important obstacle that must be overcome in order to demonstrate long-term safety of a composite femoral THR stem.

The paper by Kovacs, "*In Vitro* Studies on the Electrochemical Behavior of Carbon Fiber Composites," and the paper by Salzstein and Moran, "Stability of Polysulfone Composite Materials in a Lipid Environment," show that biocompatibility must be a two-way street. Not only must the body be able to tolerate the presence of the implant, but the implant materials must be able to survive the environment of the body. The environment of the body is uniquely dynamic and aggressive, in part because of the body's effort to biochemically isolate and/or remove foreign materials. Polymers and polymer composites have not been used extensively in structural applications in the body. These papers cover two different possibilities of human body/composite material interaction that must be evaluated to provide a reasonable level of confidence that a composite material can survive in harmony with the body in a long-term application.

The paper by Cheal, Grierson, Reilly, Sledge, and Spector, "Comparative Study of Carbon Polymer Composite and Titanium Femoral Stems in Dogs Using Computed Tomography," covers yet another important viewpoint of testing that must be performed to demonstrate the safety and potential effectiveness of composite materials in orthopaedic application. Animal studies have long been used to evaluate clinical concepts prior to use in the human body. The ability to use computed tomography (CT) to evaluate the response of bone to more elastic prostheses will permit more efficient use of animal studies in evaluating composite materials.

Since composite materials are custom engineered, theoretical analysis is an important stage in the design of the composite material. In the paper by Latour and Zhang, "The Effect of Interfacial Bonding Upon Compressive Strength and Fracture Energy of Carbon Fiber Reinforced Polymer (CFRP) Composite: A Theoretical Investigation," it is shown that micromechanical modeling of the material and its response to the mechanical load environment in the body is an important step in the design of an appropriate composite material for human body application. The paper by Liao and Reifsnider, "A Life Prediction Model for Fatigue Loaded Composite Femoral Prosthesis," demonstrates an important micro-mechanical modeling technique that can be used to evaluate the unique cumulative damage that can occur with a composite material, and its potential effect on the long-term performance of a composite prosthesis.

The paper by Zimmerman, Boone, Scalzo, and Parsons, "A Mechanical and Histological Analysis of the Bonding of Bone to Hydroxylapatite/Polymer Composite Coatings," attempts to evaluate one of the unique problems that may occur with composite prostheses, that of attachment to the tissue. In order for a composite structural prosthesis to perform as a natural part of the composite structure of the body, it must have some form of attachment to the human body. In some applications, simple direct apposition may not be sufficient and creation of an attachment interface may be necessary. Many of the methods that are used for attachment of metallic prostheses may not be suitable for composite prostheses, and consequently, new methods of attachment must be developed. This paper discusses some of the concerns that must be addressed in evaluating potential attachment interfaces both biologically and mechanically.

The paper by Hawkins, Zimmerman, Parsons, Langrana, and Lee, "Environmental Effect on a Thermal Plastic Elastomer (TPE) for Use in a Composite Intervertebral Disk Spacer," covers a unique definition of composite material in a quasi-structural application. This composite prosthesis is actually a polymer/polymer composite and represents an entirely different mechanical property problem than would be addressed by most other orthopaedic composite prostheses. The ability of the human spinal disk to repeatedly deform and recover in the human body, is an extremely difficult application for an artificial material to mimic. This paper addresses concerns and problems that must be dealt with in such an application.

The paper by Vaidyanathan, Vaidyanathan, and Waknine, "Characterization and Optimization of Small Particle Dental Composites," covers an area of composite material use in the body that is already significant. The use of composite materials in dental fillings is growing, and despite the fact that replacement of fillings in teeth is not a major operation, the long-term viability of such composite materials is important for optimization of those materials. The paper covers many of the unique mechanical and environmental tests and considerations that must be made in evaluating such materials.

Russell D. Jamison,
Smith & Nephew Richards, Inc.; Memphis, TN; symposium chairman.

Leslie N. Gilbertson
Zimmer, Inc; Warsaw, IN; symposium co-chairman.

Edward J. Cheal,[1] Anita E. Grierson,[1] Donald T. Reilly,[2] Clement B. Sledge,[2] and Myron Spector[2]

Comparative Study of Carbon Polymer Composite and Titanium Femoral Stems in Dogs Using Computed Tomography

REFERENCE Cheal, E. J., Grierson, A. E., Reilly, D. T., Sledge, C. B., and Spector, M., **"Comparative Study of Carbon Polymer Composite and Titanium Femoral Stems in Dogs Using Computed Tomography,"** *Composite Materials for Implant Applications in the Human Body: Characterization and Testing, ASTM STP 1178,* Russell D. Jamison and Leslie N. Gilbertson, Eds., American Society for Testing and Materials, Philadelphia, 1993, pp. 4–16

ABSTRACT: Clinical evaluations of canal-filling, uncemented, femoral stems continue to reveal a loss of density and thickness of the cortex of the proximal femur, consistent with a stress-shielding process. This finding has stimulated interest in the implementation of more flexible carbon fiber-reinforced polymer (CFRP) composite devices. In this study, unilateral total hip arthroplasty was performed on 34 canines using CFRP or geometrically identical titanium alloy femoral endoprostheses for periods of 6, 12, or 24 months. The CFRP composite stems had approximately one-half the bending stiffness of the metallic controls. The collarless, straight stems had a canal-filling design developed expressly for dogs. The prostheses were uncoated, with a relatively smooth surface, and were implanted with a press-fit. Computed tomography (CT) was used to quantify the remodeling of bone around the implants. With calibration of the CT images, we were able to calculate material and structural properties of the bone around the implants and in the contralateral femora, including the bone cross-sectional area and apparent density. To date, 6 of the 34 animals suffered fracture of the proximal femur. In the present investigation, CT analyses were performed on the remaining animals that were sacrificed after 6 or 12 months (a total of 20 animals). The results of these analyses indicated marked new bone formation with an increase in the quantity of radiodense bone, especially in the femoral metaphysis, and around the distal end of the stem. However, the mean bone density decreased due to the lower density of the newly formed bone, with a trend of more normal bone density at 12 months in comparison to 6 months after surgery. The occurrence of fractures and the observed remodeling suggest that the stresses in the proximal femur were relatively high, most likely due to the smooth-surfaced, press-fit, canal-filling design of the endoprostheses. Twelve months after surgery, the bone remodeling around the CFRP prostheses was not significantly different than the remodeling around the titanium alloy devices. The remodeling response could best be described as a redistribution of bone that was probably not yet complete even after 12 months. Longer-term results might reveal differences in the homeostatic structure of bone around the metallic and more flexible composite stems.

KEY WORDS: carbon, implants, femur, arthroplasty, bone, remodeling

[1]Assistant professor of Orthopaedic Surgery, Biomechanics, and research engineer, respectively, Harvard Medical School, Rehabilitation Engineering R & D, West Roxbury Veterans Administration (VA) Medical Center, West Roxbury, MA 02132.

[2]Assistant professor of Orthopaedic Surgery, chairman, and director of Orthopaedic Research, respectively, Brigham & Women's Hospital, Department of Orthopaedic Surgery, Harvard Medical School, Boston, MA 02115.

Interest in carbon-fiber reinforced polymeric (CFRP) composite materials for the fabrication of flexible femoral stems for total hip replacement prostheses [*1-3*] has been stimulated by concerns about the loss of bone mass under rigid metallic fracture-fixation plates [*4-7*] and around femoral endoprostheses [*8-12*]. In the case of metallic femoral stems, this bone loss was attibuted to stress shielding because of its association with the stiffness of the device [*10*]. The mismatch in modulus of elasticity (and stiffness) between the metallic device and the bone results in relatively little stress (strain), transmitted to certain regions of the bone, leading to atrophy. Interest in polymer composites has also been prompted by continuing concerns about the long-term biological response to metal ions released from uncemented prostheses, particularly in younger patients [*13,14*].

Glass, aramid, and quartz fibers have been considered as well as carbon fibers for the fabrication of composite materials. While thermosetting polymers such as epoxies were the earliest choices as matrix material for nonmedical applications (for example, aerospace applications), concerns about toxic effects of unreacted monomer have directed attention toward thermoplastic polymers for implant applications in surgery. Polymers undergoing investigation as matrix materials for composites for orthopedic applications include polysulfone and poly(aryletherketone) [*3,15*]. Composite materials can be formulated using (a) sheets if fibers preimpregnated with polymer; (b) polymer-impregnated tows, weaves, and braids of fibers; (c) polymer powder impregnated fibers or comingled forms; (d) discontinuous fiber sheets and split tapes; (e) carbon felts; and (f) random fibers. A number of criteria must be satisfied in material selection, in particular, the materials should be nonallergenic, nontoxic, noncarcinogenic, chemically inert and stable, and have adequate mechanical properties and environmental durability. Several approaches can be taken in the fabrication of femoral stems from composite materials: machining from flat or curve plates, filament winding, net shape molding, and pultrusion.

Concern about agents released from the polymeric matrix of CFRP composites has led to the investigation of carbon fiber-reinforced carbon (CFRC) material produced by the pyrolysis of CFRP [*16,17*]. While it was initially considered that CFRC might have a higher fatigue strength than carbon-polymer substances, uncontrollable porosity in this material can significantly reduce the strength of CFRC structures.

While interest in composite prostheses dates back to the early 1980s, relatively few animal studies have been reported. Histological studies of CFRC femoral prostheses implanted in dogs [*18*] showed a layer of connective tissue between bone and prosthesis, much like that which occurs around a press-fit metallic stem. While remodeling of bone around the composite prosthesis was reported, it was not compared with the type of osseous response that might be expected from a stiffer endoprosthesis. An important finding was carbon particles in the joint capsule. Minute carbon particles were also found in the synovium and capsule of a CFRP femoral stem implanted in dogs in a more recent study [*2*]. However, no carbon debris was found in the regional lymph nodes or in selected end organs (including spleen, liver, and lungs). Bone ingrowth was found in the porous polysulfone coating on this particular stem design. Cyclic loading (10 million cycles at 300 N) of the CFRP stem in the canine femur did not effect the bone-prosthesis strength; the force required to remove the composite prosthesis was five times greater than that was necessary to extract the control device. It was concluded from the biological and biomechanical results that the composite prosthesis could suitably replace conventional metallic stems.

Carbon fiber-polysulfone composite stems for hemiarthroplasty were compared with titanium alloy devices in another recent canine study [*1*]. Gait analysis revealed all animals to be full weight-bearing with normal gait 30 days after surgery. Radiographically, only one of the components subsided; however, this device was found to be stabilized after 20 months. A radiodense line was noted around the component in all the animals after three months. The location of this line relative to the surface of the stem was difficult to assess because of the radiolucency of the device. Computed Tomography (CT) imaging revealed the same radiodense line and new bone formation in the form of densification of the metaphyseal cancellous bone. Microscopic examination revealed no evidence of delamination or microfracture of the prosthesis and no evidence of particle migration. Generally, there was a favorable histological response to the device. Active bone remodeling was found around the prosthesis at the dense cancellous regions and at the endosteal bone surface. It was concluded that the composite prosthesis demonstrated mechanical integrity, biocompatibility, and at the same time provoked a constructive bone remodeling response.

Investigation of the performance of composite prostheses in human subjects have been performed in Europe. In one study, 17 patients underwent surface replacement with a silicon carbide reinforced bipolar prosthesis [*19*]. In another study, CFRC femoral stems were implanted [*17*]. Unfortunately, major material-related complications were reported after a follow-up of up to two years. The clinical trial of the CFRC femoral stem [*17*] was recently discontinued.

At first glance, the results of laboratory testing and animal and clinical investigations of composite prostheses are encouraging. However, the small numbers and short time of the animal studies make it impossible to draw definitive conclusions. Further *in vivo* study is required to explore the potential of these materials in total joint replacement. The objective of the present study was to investigate the biological performance of CFRP composite stems in a canine model. Particular attention was given to comparing the structural properties between the canine and human stems and establishing geometric similitude. This is an essential (and sometimes overlooked) aspect of efficacy in animal studies. Here we report the bone remodeling response around these prostheses six and 12 months after implantation as measured by computed tomography.

Methods

To test the hypothesis that more flexible femoral stems lead to less cortical bone loss, CFRP and titanium alloy femoral stems were implanted into the right femora of 34 large hound-like dogs, weighing from 32 to 50 kg. The animals were screened radiographically for acceptable canal size. The polymer used for the CFRP stems was poly(arylетherketone). The stems were smooth-surfaced, symmetrical, collarless prostheses, designed to be canal-filling and stabilized by interference fit (Fig. 1). The CFRP stems had approximately one-half the bending stiffness of the titanium alloy controls. A cobalt-chromium alloy ball was affixed to a taper on the stem. Three different hole sizes in the balls allowed for three different neck lengths. Commercially available canine polyethylene cups were cemented into the acetabulum using conventional technique. After surgery animals were allowed to ambulate as pain permitted.

The animals were scheduled to be sacrificed after a period of six, twelve, or 24 months. The study population for this report included the animals sacrificed after six and twelve months (Table 1). All of the animals except one in the six month CFRP group received components of identical size. These femoral components had dimensions of approximately 22 (medial-lateral) by 11 mm (anterior-posterior) at the level of the medial neck cut, and a distal diameter of approximately 9 mm. The one animal that was an exception required a femoral component that was 5% smaller. A tolerance of -1 to $+1.5$ mm for the medullary canal diameter, relative to the stem diameter, was used for radiographic screening of the animals.

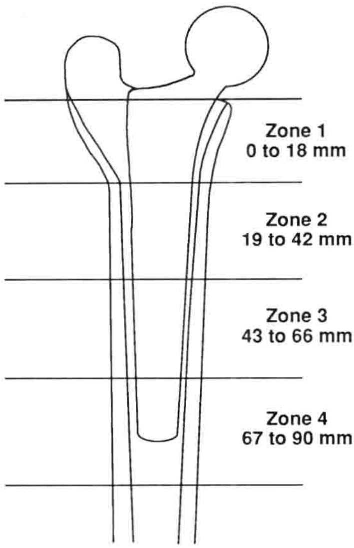

FIG. 1—*Frontal view of the canine femur and prosthesis, and zones of analysis.*

Postoperatively, the animals were evaluated clinically using gait analysis and plane film radiography. After sacrifice, the femora were scanned using quantitative CT. In addition, one dog that received a CFRP prosthesis was scanned under anesthesia six months after surgery, as well as after sacrifice at twelve months (Table 1). The scans were obtained with either a Seimens Somotom DR or a GE9800 CT scanner, depending on availability. The scan-to-scan distance was 3 mm. The CT data were transferred via magnetic tape to the laboratory computer system for quantitative analysis.

To evaluate the femoral component of the canine total hip arthroplasty as a model for the femoral component of a human total hip arthroplasty, the cross-sectional properties of the canine implant-bone composite structure were compared to the corresponding cross-sectional properties of a human implant-bone composite structure. The areas and area moments of inertia were measured from a CT scan 1.5-mm distal to the lesser trochanter in one of the experimental animals that received a titanium femoral component. To determine the corresponding properties in the human, a representative femur was selected from our database of women total hip arthroplasty candidates in the age range of 50 to 65 years. The selected femur was near the mean of this population in regards to the size of the femoral

TABLE 1—*Number of animals and total number of sets of CT scans at each of the two time periods. There was one more set of scans at six months than dogs sacrificed after six months since one twelve month dog was also scanned after six months.*

Stems	6 months	12 months
Dogs with CFRP stems	8	8
Dogs with titanium alloy stems	0	4
CT scans, CFRP stems	9	8
CT scans, titanium alloy stems	0	4

canal. The area and area moments were measured for a horizontal scan 3-cm distal to the lesser trochanter. The geometric properties of a prototype femoral component, designed for this human population using a custom design algorithm [*20*], were also measured at the corresponding horizontal section. The ratios of the axial and bending stiffness of the prosthesis to the axial and bending stiffness of the cortical bone were then calculated for the canine and human subjects at this horizontal cross-section.

The bone remodeling in the operated animals was measured from the CT images. To assign physical meaning to the image data, the CT numbers were converted to bone apparent density and to elastic modulus. A calibration phantom containing dipotassium phosphate (K_2HPO_4) solutions of varying concentrations was included when the bones were scanned [*21*]. Each separate image was calibrated by measuring the average CT number for each of the six chambers of the phantom, and then performing a linear regression between the CT number and the K_2HPO_4 density.

The bone tissue in the normal femur of an adult canine (or human) consists primarily of two types of bone, cortical and trabecular. These bone types are most importantly distinguished by the apparent density, and the apparent density is primarily a function of the porosity (for example, the density of the solid phase is relatively constant). The apparent density of trabecular bone generally ranges from about 0.1 to 0.9 g/mL, while the apparent density of diaphyseal cortical bone ranges from about 1.8 to 2.0 g/mL [*22,23*]. An empirical linear relationship was available to relate the calibrated CT density to the bone apparent density[3]

$$\rho = 1.618 \times 10^{-3}\, \rho_c + 5.861 \times 10^{-2}\ \text{g/mL, for } \rho < 1.0\ \text{g/mL} \tag{1}$$

where

ρ = bone apparent densiy, g/mL, and
ρ_c = K_2HPO_4 solution density, g/mL.

However, this equation was based on calibrated CT data and direct measurements of the apparent density of trabecular bone from a cadaveric human tibia, in which the apparent density of the included specimens did not exceed 0.55 g/mL. Unfortunately, we found that application of this equation to diaphyseal cortical bone resulted in an overestimate of the bone apparent density, with predicted values exceeding 2.5 g/mL. We used a second linear relationship to calculate bone apparent density for the higher density regions:

$$\rho = 1.329 \times 10^{-3}\, \rho_c + 2.269 \times 10^{-1}\ \text{g/mL, for } \rho \geq 1.0\ \text{g/mL} \tag{2}$$

This second equation was established by forcing the two linear equations (Eqs 1 and 2) to intersect at a bone apparent density of 1.0 g/mL and by forcing the second equation to produce a mean bone apparent density of 2.0 g/mL for the diaphyseal cortical bone of a sample calibrated image of a normal canine femur (avoiding the periosteal and endosteal surfaces in the sample image). The apparent density of 1.0 g/mL was used to distinguish trabecular bone (Eq 1) from more compact bone (Eq 2), the more compact bone thus including primarily cortical bone. All bone in the images that exceeded this threshold value were referred to in this paper as radiodense bone.

The right (implanted) and left (intact) femora were analyzed separately by manually defining rectangular or polygonal regions of interest in each image. The implant was

[3]Zysset, P. and Hayes, W. C., personal communication, 1990.

eliminated from analysis by the definition of a void region. The calculated parameters from each CT image included the cross-sectional area and the mean apparent density of the radiodense bone ($\rho \geq 1.0$ g/mL). The cross-sectional area was calculated by simply summing the area of all the image pixels for which this density threshold was exceeded. The mean density was calculated by calculating the average density of the same pixels. Finally, the relative values of the area and density were calculated for each image by taking the percent differences between the right (implanted) and left (intact) sides. For example

$$\text{Relative Area} = 100\% \cdot (A_r - A_l)/A_l \tag{4}$$

where

A_r = area on the right (implanted) side, mm^2, and
A_l = area on the left (intact) side, mm^2.

A similar equation was used to calculate the relative density of the radiodense bone.

To simplify interpretation and to allow comparison of the present data to those of other studies, the results for multiple images were combined based on four geometric zones (Fig. 1). The four zones corresponded to the proximal stem (the femoral metaphysis), the proximal mid-portion of the stem, the distal mid-portion of the stem, and the distal end of the stem. The latter zone (zone 4) included several images of each femur distal to the end of the stem. Means were calculated for the images in each zone, for each animal. The overall mean and the standard deviation of this mean were then calculated for each zone, for each of the three experimental groups (CFRP stem at six months, CFRP stem at twelve months, and titanium alloy stem at twelve months). Finally, unpaired t tests were performed for each parameter and each zone, using the means from each animal, to test for significant differences between the six and twelve month CFRP groups, and between the twelve month CFRP and twelve month titanium alloy groups. In other words, the overall mean, standard deviation, and unpaired t tests were calculated using the individual means, not the individual scans that produced those means. The group differences were considered statistically significant if $p < 0.05$ from the unpaired t tests.

Results

The cross-sectional analysis of the canine and human femora demonstrated very close correspondence for the stiffness of the prosthesis relative to the stiffness of the bone (Table 2). These calculations were performed for titanium femoral components at a section through the proximal diaphysis. The axial stiffnesses of the human stem and femur were approximately two times greater and the bending stiffnesses were approximately four times greater than those of the canine. Most importantly, the ratio of the axial stiffness of the prosthesis to the axial stiffness of the femur was 3.65 for the canine animal model and 3.55 for the post-menopausal woman with a stem that was designed to be canal-filling. Similarly, the ratio of the bending stiffness of the prosthesis to the bending stiffness of the femur was 0.92 for the canine animal model and 0.86 for the same human and stem.

At present, nine of the thirty-four operated animals have been lost to the study. One of these nine died during surgery related to anesthesia and one died six weeks after surgery due to liver disease. The remaining seven had complications related to the arthroplasty, one suffering a dislocation, and six suffering fracture of the femoral metaphysis. These seven animals were euthanized prematurely and were excluded from further analysis.

TABLE 2—*Comparison of the stiffnesses of the human and canine titanium endoprostheses and the cortical bone at a section through the proximal diaphysis.*

Parameter	Axial,[a] MN		Bending,[b] N·m²	
	Human	Canine	Human	Canine
Stem[c]	26.28	12.28	544.3	139.9
Femur[d]	7.39	3.37	633.3	152.1
Ratio[e]	3.55	3.65	0.86	0.92

[a]The axial stiffness was equal to the product of the elastic modulus and the cross-sectional area.
[b]The bending stiffness was equal to the product of the elastic modulus and the maximum principal moment of inertia.
[c]An elastic modulus of 18 GPa was assumed for the cortical bone of the human and canine femora.
[d]An elastic modulus of 110 GPa was assumed for each stem (titanium alloy).
[e]The ratio was equal to the stiffness of the stem divided by the stiffness of the femur (dimensionless).

None of the fractures were apparent at the time of surgery or in the first post-operative radiographs. However, three of the fractures were apparent in radiographs taken six or eight days after surgery. The other three fractures did not appear until four to seven weeks after surgery. All six femoral fractures occurred in animals that received CFRP composite prostheses; thus the frequency of fracture for the CFRP stems was 6 of 28 and the frequency of fracture for the titanium alloy stems was 0 of 6 (the additional animals not included in Table 2 were scheduled for sacrifice at 24 months and all animals without fractures were at least one year post-surgery). However, based on a chi-square analysis, the null hypothesis that the occurrence of fracture is independent of the prosthesis material cannot be rejected ($p = 0.51$).

The operated animals included in the present analyses appeared to ambulate normally after a brief recovery period. The general trend from the force plate data was that at six months the operated limb was loaded to approximately 50 to 75% of the unoperated limb, while the dogs at one year showed mostly equal weight bearing. No statistically significant differences in the force ratios were found between the experimental groups. Exposure of the hip joint after sacrifice did not reveal the presence of carbon debris or any untoward response.

Radiography revealed the presence of a thin radiodense line at a location consistent with the CFRP bone interface. Visualization of this radiographic feature was enabled by the radiolucency of the composite stem. An increase in the density of bone within the medullary canal at the distal tip of the CFRP and titanium alloy stems also was apparent. The severe cortical thinning and increase in porosity found around titanium stems in other studies employing a canine animal model [*24*] was not seen in the plane film radiographs.

Based on the quantitative CT analyses, a significant increase in the total quantity of radiodense bone ($\rho \geq 1.0$ g/mL) occurred in the proximal femoral metaphysis and around the distal end of the stems, in support of our observations from the plane film radiographs (Fig. 2). The most proximal scans were just distal to the medial surgical cut (the most proximal scans in which the stem was surrounded by bone), and were assigned as the origin (0 mm). The distal end of the prosthesis was at a scan level of approximately 75 mm. The increase relative to the left (intact) femora generally peaked near the most proximal sections and just distal to the tip of the stem.

The relative quantity of radiodense bone in each of the four zones varied between the different experimental groups (Table 3 and Fig. 3). The quantity of bone in the twelve month CFRP group tended to be closer to normal (closer to the contralateral femur, and

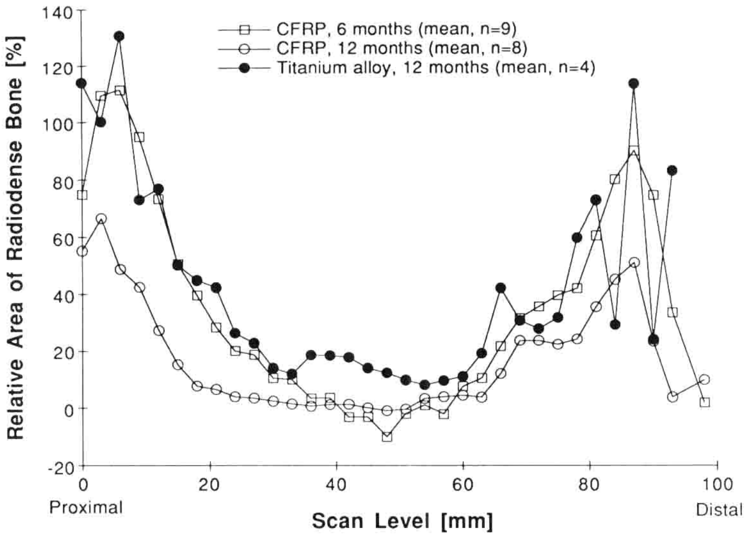

FIG. 2—*Cross-sectional area of radiodense bone* (ρ ≥ *1.0 g/mL) in the femur with the prosthesis as a percentage difference from the corresponding area in the contralateral femur (Eq 4). The data were averaged at each scan level over all animals in each group. The distal tip of the stem was at a scan level of approximately 75 mm.*

thus a relative value closer to zero) than both the six month CFRP group and the twelve month titanium alloy group. However, based on the unpaired *t* tests of each zone, these differences did not reach statistical significance.

The mean density of the radiodense bone around the implants was significantly less than the corresponding density of the contralateral femora (Table 4 and Fig. 4). The mean density around the titanium alloy stems and the CFRP stems at twelve months was approximately 5% less than the density of the contralateral femora. However, the density around the CFRP stems at six months was closer to 10% less than the density of the contralateral femora. At zone 1, this difference between the six and twelve month CFRP groups was statistically significant.

TABLE 3—*Means (and standard deviations) of the areas of radiodense bone in each zone of the canine femora, in mm². In all cases, the CFRP composite or titanium alloy femoral component was implanted in the right femur, and the left femur was left intact.*

Zone	Side	CFRP, 6 month (n = 9)	CFRP, 12 month (n = 8)	Ti, 12 month (n = 4)
1	right	195.85 (45.76)	174.38 (38.66)	254.99 (60.38)
	left	111.64 (6.68)	128.52 (32.55)	151.48 (28.34)
2	right	139.97 (22.80)	135.43 (30.46)	170.64 (26.88)
	left	125.83 (11.74)	136.92 (31.30)	151.52 (21.01)
3	right	124.64 (21.76)	121.49 (30.52)	154.17 (18.13)
	left	120.52 (8.56)	124.51 (24.99)	140.89 (19.81)
4	right	158.91 (47.85)	147.88 (43.70)	174.81 (19.42)
	left	114.99 (9.14)	121.83 (16.71)	132.48 (14.83)

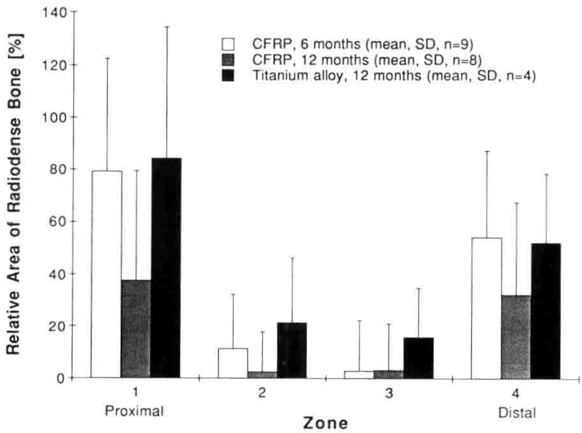

FIG. 3—*Mean and standard deviation (SD) of the cross-sectional area of the radiodense bone* ($\rho \geq 1.0$ *g/mL) in the femur with the prosthesis as a percentage difference from the corresponding area in the contralateral femur (Eq 4). The means for each zone were averaged over all animals in each group.*

Discussion

We employed a canine animal model to test the application of a CFRP composite to the femoral component of total hip arthroplasty. To evaluate the relevance of this animal model, we compared the mechanical stiffnesses of the femoral stems relative to that of the canine and human femora, respectively, at a cross-section just distal to the lesser trochanter of each femur. The ratio of the axial and bending stiffnesses of the prosthesis to the cortical bone of the femur were in good agreement between the canine and human. Note that the particular human implant was of contemporary design, and relatively canal-filling. A more complete comparison of the mechanics of the human and canine femora requires knowledge of the complex loads acting at the particular cross-section, and is beyond the scope of this paper. While the present comparison does not account for other differences in anatomy or especially functional loads, it does provide partial support of the present animal model for the testing of alternative materials for femoral endoprostheses.

We used plane film radiography, gait analysis, and CT image analysis to evaluate the performance of the CFRP composite prosthesis relative to the performance of a similar

TABLE 4—*Means (and standard deviations) of the density of radiodense bone in each zone of the canine femora, in g/mL. In all cases, the CFRP composite or titanium alloy femoral component was implanted in the right femur, and the left femur was left intact.*

Zone	Side	CFRP, 6 month (n = 9)	CFRP, 12 month (n = 8)	Ti, 12 month (n = 4)
1	right	1.36 (0.06)	1.44 (0.06)	1.54 (0.09)
	left	1.52 (0.12)	1.57 (0.08)	1.68 (0.16)
2	right	1.54 (0.09)	1.62 (0.08)	1.70 (0.12)
	left	1.70 (0.13)	1.75 (0.08)	1.83 (0.17)
3	right	1.61 (0.11)	1.69 (0.12)	1.72 (0.13)
	left	1.76 (0.12)	1.80 (0.07)	1.86 (0.17)
2	right	1.54 (0.12)	1.65 (0.11)	1.65 (0.14)
	left	1.74 (0.12)	1.79 (0.08)	1.82 (0.17)